

Fast Imaging in Flow: A Means of Combining Flow-Cytometry and Image Analysis

V. KACHEL, G. BENKER, K. LICHTNAU, G. VALET AND E. GLOSSNER

Max-Planck-Institut für Biochemie, D8033 Martinsried, W-Germany

Received for publication June 13, 1978

The morphological identification of cells by flow cytometry is difficult. Usually cell sorting and microscopical analysis have to be used in addition. Morphological analysis is simplified by taking cell pictures from a range of particular interest immediately during flow cytometric analysis. Instruments using the video scanning technique for fluorescence imaging are slow and expensive (8, 10). Morphological information can also be obtained by transmission imaging of cells in flow, which requires shorter exposure times. Therefore a cell volume activated flow imaging device has been developed which operates at flow speeds up to 5 m/sec and which depicts transmission images of selected cells on a 16-mm film by a nsec flashlamp illumination. An electronic unit detects the particles in the optically accessible orifice, performs the pulse height analysis, triggers the flashlamp if particles are in the preselected range of interest and feeds the film. The instrument is capable of delivering up to 150 pictures per second and works either as a flow microscope in which the cells in the preselected volume range are directly observed, or as a picture storage system in which the cell pictures are stored on the 16-mm film for documentation or for image analysis.

Two qualitatively different methods for automatic cytometry are presently available. The method of image analysis is capable of providing information on the structure and shape of cells and their nuclei as well as on the local distribution of substances within the cell or on its surface membrane. The limitation of these methods is that only a few of cells prepared on microscope slides can be evaluated per time. The flow-through principle, however, permits measurements of many cells over the same period of time, but morphological resolution is mostly impossible.

A combined application of both methods seems to be ideal because flow cytometric measurements allow a quick preselection of cells from a large sample and cells of a special interest may be analyzed thoroughly by the image analysis method.

Here we report on our attempts to combine the two methods. Cells of a particular volume were preselected by the resistance pulse flow method and pictures of these cells taken immediately during the volume analysis were recorded by photographic means for subsequent morphological analysis.

MATERIALS AND INSTRUMENTATION

General principles and basic instrumentation: The cells are analyzed according to their volume by the resistance pulse technique (Metricell principle) (4, 6). The cells, positioned near the axis of the orifice by hydrodynamic focusing, move with velocities between 3 and 5 m/sec. A Zeiss Universal microscope with a 40×0.75 water immersion objective and a beam switch head is used as basic optical equipment (Zeiss, Oberkochen, W-Germany). A Metricell type current supply and Metricell amplifiers deliver the volume pulses which are analyzed by a Tracor NS 633 pulse height analyzer. The nanosecond flashlamp device (Nanolite Nr. 177 flashtube and Nanolite driver, Impulsphysik, Hamburg) is described in Reference 4.

The optically accessible transducer: The proper transducer chamber is similar to that used in (5) and consists of a plexiglass disc with two cavities containing the platinum foil electrodes (9). In the center of the disc the cavities narrow down to a minimal distance of 80 to 100 μm (Fig. 1). At this point both cavities are connected by a rectangular channel of 60 to 120 μm depths and width which is cut into the wall between them. This channel forms the orifice in which measuring and photographing of the cells take place. The front side of the chamber and of the orifice is covered by a cover glass that is fixed by a pressing screw. Details of the fluid system are shown in Figure 2.

The trigger device: The light flash used to photograph the cell in the orifice has to be triggered while the cell is inside the orifice, but the decision to photograph the cell or not can first be made when the pulse maximum is reached. The pulse maximum, which contains the cell volume information, appears when the cell is in the central plane of the orifice (point *B* of Fig. 3). The cells leave the orifice at the 80% point *C* and thus only the time between *B* and *C* is available for photographing the cells inside the orifice. The high voltage spark discharge of the flashlamp distorts the volume pulses. Consequently either the pulse height analysis, or the pulse height transfer to the analyzer, has to be completed (point *B'*) and the flash activated in the time between *B'* and *C*. The region of interest is selected by an amplitude window with adjustable center and width. Pulse height transfer and flash activation are disabled if the pulse maximum is outside the window. A "window off" switch enables the display of the complete pulse height distribution at the screen of the pulse height analyzer.

The camera and control unit: Camera and control unit are of our own design (1). The camera uses a commercial Arriflex cassette (Arnold und Richter, München) to support the 16-mm Eastman Plus-X and Double-X negative film (Fig. 4). It is equipped with two independent electric motor drives, one step motor for transporting the film through the picture gate and a direct current motor for supporting the film. The film is buffered between the two drives by a loop. The length of the loop is controlled by an infrared light barrier.

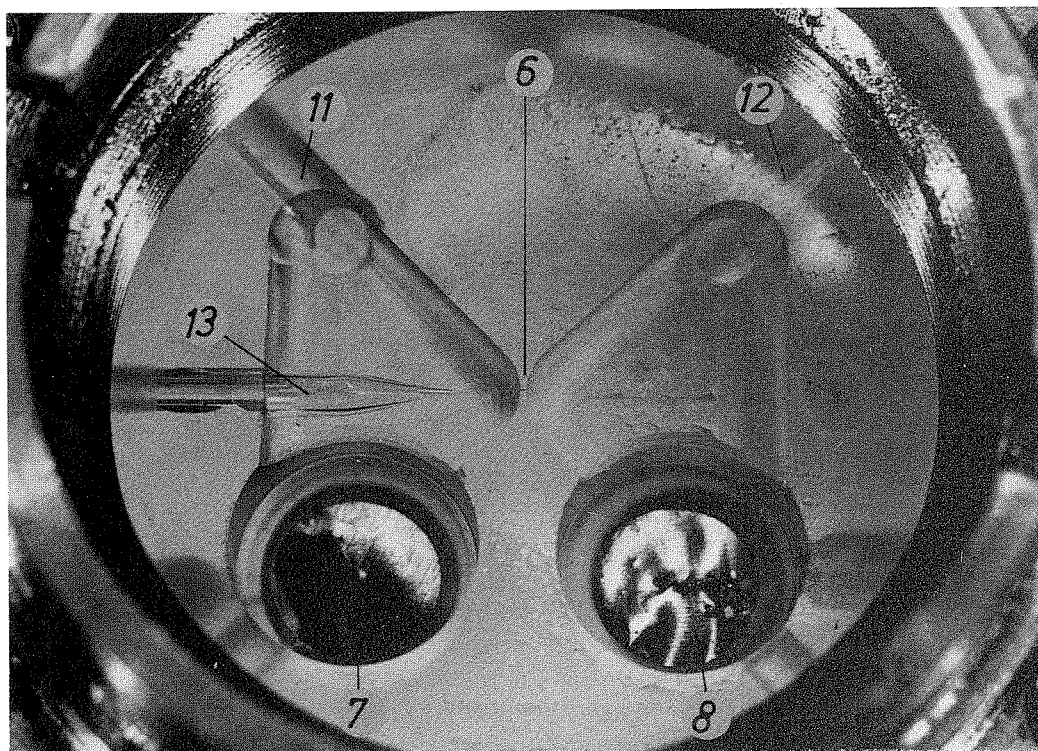


FIG. 1. The transducer chamber (explanations, Fig. 2).

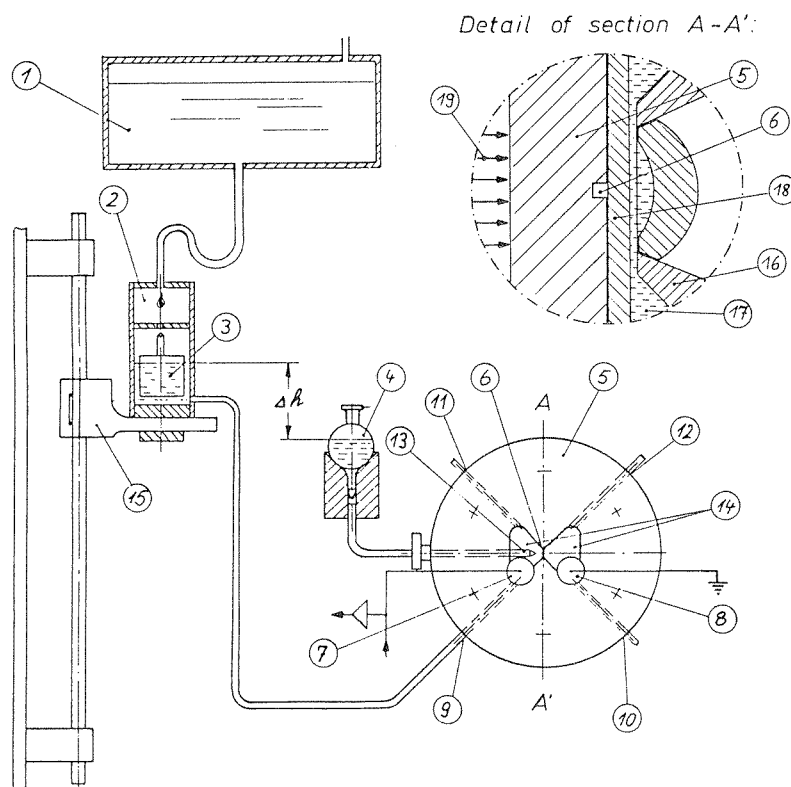


FIG. 2. Schematic diagram of the fluid system. 1, electrolyte tank; 2, dropping chamber; 3, regulating chamber; 4, particle container; 5, plexiglass disk; 6, orifice; 7 and 8, electrodes; 9, supply tube of particle-free electrolyte; 10, cleaning tube; 11, breather tube; 12, suck connection; 13, particle injector; 14, cavities; 15, moveable particle injection control; 16, objective; 17, immersion; 18, cover glass; 19, illumination;

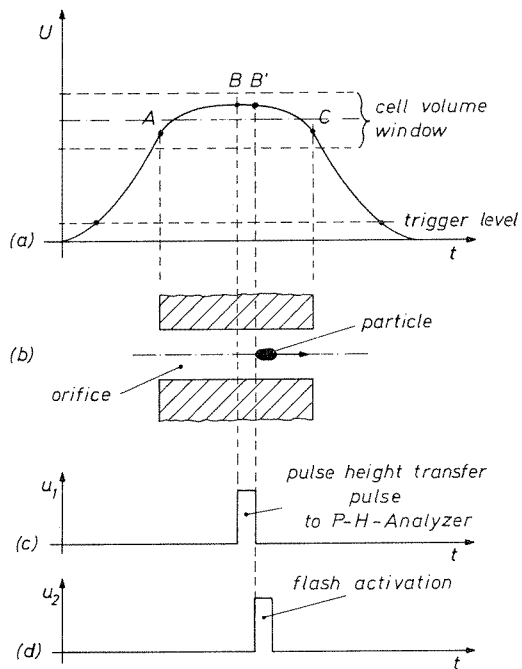


FIG. 3. Time conditions for the flash activation. A, particle entering point (80% pulse height); B, pulse maximum containing the volume information; B-B', pulse height transfer time; C, particle leaving point (80%). The time between A and C is 10 to 20 μ sec depending on the pressure difference and the orifice geometry.

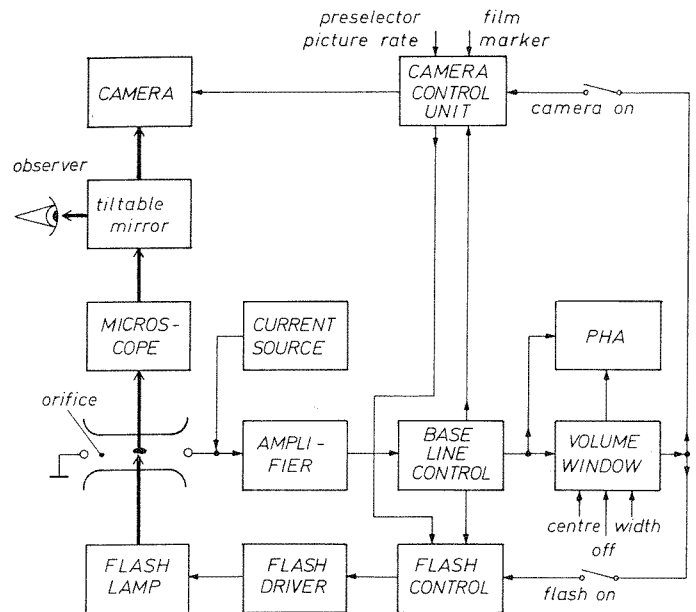


FIG. 5. Block diagram of the complete flow imaging device. The thick lines indicate optical pathways.

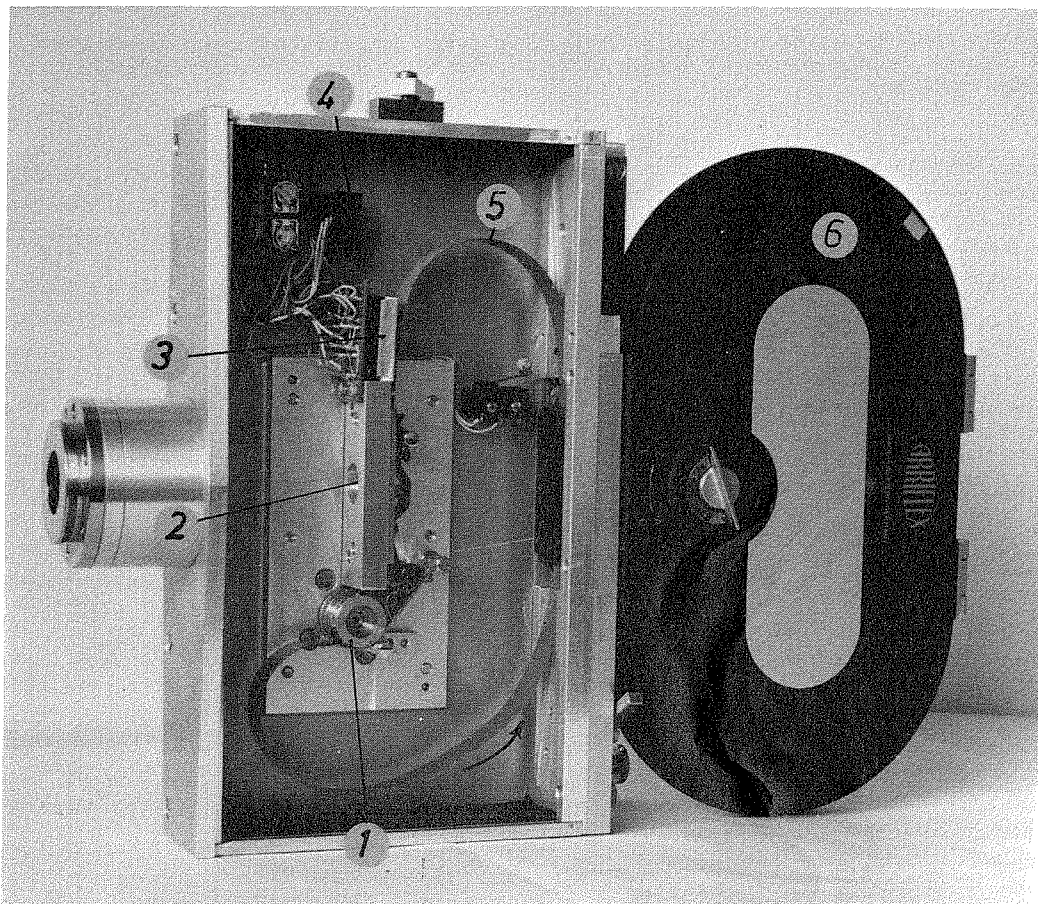


FIG. 4. The camera with Arriflex cassette. 1, sprocket, driven by the step motor; 2, picture gate; 3, three digit hexadecimal film marker; 4, infrared light barrier for controlling the film loop; 5, film loop; 6, Arriflex cassette; the direction of the film motion is indicated by the arrow.

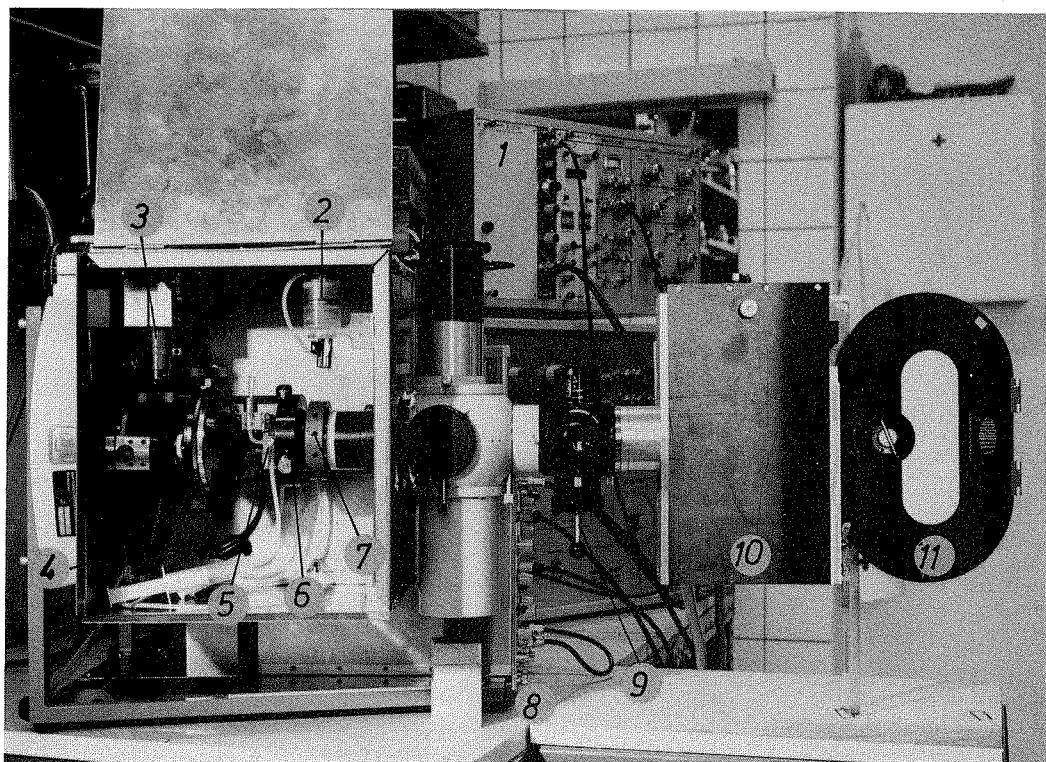


FIG. 6. The flow imaging prototype. 1, pulse height analyzer; 2, regulating chamber for controlling the particle rate; 3, flash tube; 4, shielding cage; 5, transducer chamber; 6, adjustment screws; 7, focusing screws; 8, current source and amplifiers; 9, beam switch; 10, camera; 11, cassette supplying and winding up the film.

The control unit supervises the camera and the flash generation. It is triggered by the random arrival of cells in the orifice. The film is advanced after each flash by three motor steps. A picture rate preselector limits the maximum picture rates to between 2 and 150/sec. On a normally used 30-m film 4000 pictures are stored. Cell pictures of different samples on the same film are identified by a three digit hexadecimal number. Three counters count and display the total number of measured cells, the cell in the selected window and the number of cells stored on the film. In the case of baseline distortions of the volume pulses, the pulse height analysis, film transport and activation of the flash are interrupted.

The complete device: Figure 5 shows a block diagram and Figure 6 shows a photograph of the imaging device.

RESULTS AND DISCUSSION

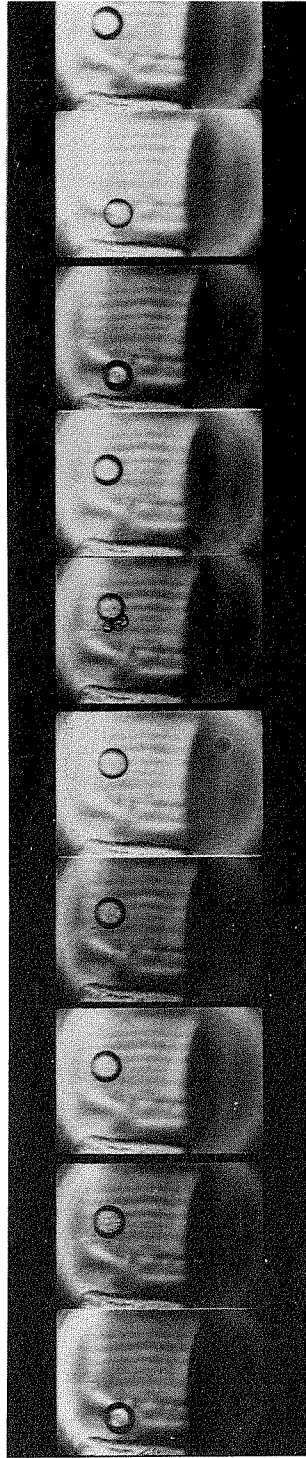
First examples of application: Figure 7(a) shows the volume distribution curve of 20 μm mean diameter latex particles measured with the imaging chamber. The particles that are depicted in Figure 7(b) are selected from the right slope of the distribution curve. Cell aggregation can be determined quantitatively by the resistance pulse technique. Erythrocyte aggregation is correlated with the risk factors of myocardial infarction (2). The fast imaging in flow device offers a means of differentiating between real cell aggregates and groups of cells disrupted by the flow forces but passing as apparently coincident cells through the orifice. Figure 8(a) shows a volume distribution curve of singlets and multiplets of human erythrocytes. The doublets photographed in Figure

8(b) correspond to the second peak of the distribution curve and the triplets of Figure 8(c) correspond to the third peak of the distribution curve. The cells are measured in dextran T250 2.5%.

Further development aims: Figures 7 and 8 indicate that all cells are not yet in focus. Therefore the cells must be better stabilized in the optical focus plane by improved hydrodynamic focusing. The height of the volume pulses depends on the current density in the channel. In the present chamber, current is short circuited in the electrolyte layer between the plexiglass disc and the coverglass and thus the pulse height is reduced. This instable current loss must be avoided. The optical quality can be improved by use of more intense light flashes. Chambers with lateral cell orientation will be developed (3, 7), and fluorescence and multiparameter signals will be used for mapping in flow.

LITERATURE CITED

1. Benker G: Entwurf und Aufbau einer elektronisch gesteuerten Bildaufzeichnungseinheit für Aufnahmen von biologischen Zellen in einem Durchflußzytometer Diplomarbeit Technische Universität München 1978
2. Boss N, Koenig S, Ruhlenstroth-Bauer G: The red blood cell aggregation in men with coronary risk factors. *Klin Wochenschr* 53:358, 1975
3. Dean PN, Pinkel D, Mendelsohn ML: Hydrodynamic orientation of sperm heads for flow cytometry. *Biophys J* in press
4. Kachel V: Methoden zur Analyse und Korrektur apparativ bedingter Meßfehler beim elektronischen Verfahren zur Teilchen-



(b)

(a)

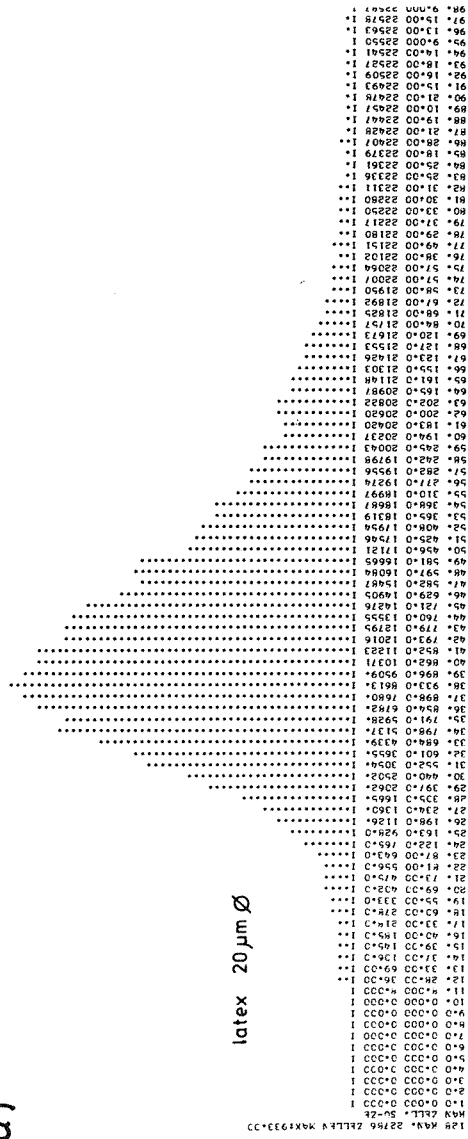


Fig. 7. (a), Volume distribution curve of 20 μm mean diameter latex particles measured with the imaging chamber. Channel width 120 μm. (b), Sequence of particles selected from the right slope of the distribution curve (large particles). Flow direction from bottom to top.

DATA: 110422

128 KAN, 22786 ZELLEW MAR1933.CC

MAR ZELLE, SU-ZE

1.0	0.000	0.000	1
2.0	0.000	0.000	1
3.0	0.000	0.000	1
4.0	0.000	0.000	1
5.0	0.000	0.000	1
6.0	0.000	0.000	1
7.0	0.000	0.000	1
8.0	0.000	0.000	1
9.0	0.000	0.000	1
10.0	0.000	0.000	1
11.0	4.000	4.000	1
12.0	28.000	30.000	1
13.0	33.000	69.000	1
14.0	37.000	106.000	1
15.0	39.000	145.000	1
16.0	40.000	185.000	1
17.0	33.000	214.000	1
18.0	63.000	218.000	1
19.0	65.000	333.000	1
20.0	69.000	422.000	1
21.0	73.000	475.000	1
22.0	81.000	526.000	1
23.0	87.000	643.000	1
24.0	122.000	755.000	1
25.0	163.000	928.000	1
26.0	196.000	1126.000	1
27.0	236.000	1360.000	1
28.0	259.000	1665.000	1
29.0	297.000	2062.000	1
30.0	440.000	2502.000	1
31.0	501.000	3056.000	1
32.0	601.000	4332.000	1
33.0	684.000	5137.000	1
34.0	998.000	5137.000	1
35.0	991.000	5928.000	1
36.0	956.000	6782.000	1
37.0	898.000	7680.000	1
38.0	831.000	8613.000	1
39.0	866.000	9509.000	1
40.0	862.000	10371.000	1
41.0	852.000	11283.000	1
42.0	793.000	12016.000	1
43.0	779.000	12795.000	1
44.0	760.000	13535.000	1
45.0	721.000	14278.000	1
46.0	629.000	14905.000	1
47.0	582.000	15487.000	1
48.0	591.000	16084.000	1
49.0	581.000	16685.000	1
50.0	526.000	17121.000	1
51.0	425.000	17566.000	1
52.0	368.000	18139.000	1
53.0	360.000	18619.000	1
54.0	310.000	18997.000	1
55.0	277.000	19274.000	1
56.0	282.000	19526.000	1
57.0	282.000	19526.000	1
58.0	242.000	19798.000	1
59.0	194.000	20237.000	1
60.0	183.000	20420.000	1
61.0	200.000	20820.000	1
62.0	202.000	20822.000	1
63.0	165.000	20987.000	1
64.0	161.000	21148.000	1
65.0	150.000	21303.000	1
66.0	123.000	21426.000	1
67.0	127.000	21533.000	1
68.0	127.000	21533.000	1
69.0	66.000	21757.000	1
70.0	66.000	21757.000	1
71.0	68.000	21825.000	1
72.0	67.000	21825.000	1
73.0	58.000	21950.000	1
74.0	57.000	22007.000	1
75.0	57.000	22007.000	1
76.0	58.000	22102.000	1
77.0	49.000	22151.000	1
78.0	29.000	22180.000	1
79.0	31.000	22217.000	1
80.0	33.000	22250.000	1
81.0	30.000	22280.000	1
82.0	31.000	22311.000	1
83.0	25.000	22336.000	1
84.0	25.000	22361.000	1
85.0	18.000	22379.000	1
86.0	21.000	22402.000	1
87.0	19.000	22447.000	1
88.0	19.000	22447.000	1
89.0	10.000	22487.000	1
90.0	21.000	22476.000	1
91.0	15.000	22493.000	1
92.0	18.000	22509.000	1
93.0	18.000	22527.000	1
94.0	14.000	22541.000	1
95.0	9.000	22550.000	1
96.0	13.000	22543.000	1
97.0	19.000	22528.000	1
98.0	9.000	22547.000	1

- größenbestimmung nach Coulter. Thesis Technische Universität Berlin, D83 1972
5. Kachel V: Methodology and results of optical investigations of formfactors during the determination of cell volumes according to Coulter. *Microsc Acta* 75:419, 1974
 6. Kachel V: Basic principles of electrical sizing and their realization in the new instrument Metricell. *J Histochem Cytochem* 24:211, 1976
 7. Kachel V, Kordwig E, Glossner E: Uniform lateral orientation, caused by flow forces, of flat particles in flow through systems. *J Histochem Cytochem* 25:774, 1977
 8. Kay DB, Cambier JL, Wheeless LL: Imaging in flow. Vith Engineering foundation conference on automated Cytology Schloß Elmau Abstr. Vol 6, 1978
 9. Lichtnau K: Aufbau eines kombinierten Zellvolumen-Zellabsorptions-Meßgerätes nach dem Durchflußprinzip. Ingenieurarbeit, Fachhochschule, München, 1978
 10. Wheeless LL, Kay DB, Cambier MA, Cambier JL, Patten SF: Imaging system for correlation of false alarms in flow. *J Histochem Cytochem* 26:864, 1977

